Probing Long-Range Coulomb Interactions in Nanoscale MOSFETs

Ming-Jer Chen, *Senior Member, IEEE*, Li-Ming Chang, *Student Member, IEEE*, Sih-Yun Wei, Wan-Li Chen, Ting-Hsien Yeh, Chuan-Li Chen, and Yu-Chiao Liao

***Abstract*— We have recently experimentally probed long-range Coulomb interactions due to plasmons in polysilicon gate of long-channel (1 μm) MOSFETs. In this letter, we further probe those due to plasmons in the highly doped source and drain. Test vehicles include four more samples from the same manufacturing process but with small channel lengths (down to 33 nm). I–V's of devices are measured at two drain voltages of 0.05 and 1 V, in a temperature range of 292–380 K. Inverse modeling technique is applied to furnish calibrated doping profiles. The inversion layer electron effective mobility is thereby extracted, showing a decreasing trend with decreasing channel length. Such differences reflect more additional scatterers in the shorter devices. Mobility components limited by these additional scatterers are assessed using Matthiessen's rule. From the extracted temperature dependencies, we infer that the strength of source/drain plasmons increases with decreasing channel length. The errors of Matthiessen's rule are adequately dealt with. Corroborative evidence is given as well.**

***Index Terms*— Device physics, long-range Coulomb, MOSFETs, mobility, plasmons, scaling, scattering, transport.**

I. Introduction

FOR doped semiconductors, there are quantized collective modes of electrons in the context of many-body theory, namely, plasmons [1]. The existence of plasmons means the occurrence of long-range Coulomb interactions not only within, but also outside doped regions of semiconductor devices. Thus, for state-of-the-art MOSFETs at the nanometer dimension, electrons traveling in the channel will undergo long-range Coulomb interactions with plasmons in the highly doped source and drain [2]. Through sophisticated simulation tasks [2]–[4], such long-range Coulomb interactions are shown to act as key limiting factors in MOSFETs scaling.

Experimentally probing long-range Coulomb interactions in realistic devices are a highly challenging issue [5]. We have recently successfully reached this through extracted mobility limited by interface plasmons in polysilicon ultrathin gate oxide [6]. Those due to source/drain plasmons may be assessed from the observed mobility degradation with decreasing gate length [7]–[9], as long as other scattering mechanisms have been distinguished in advance. In doing so, Matthiessen's rule can be helpful, but care must be taken [10]–[12].

Manuscript received October 3, 2013; revised October 10, 2013; accepted October 16, 2013. Date of publication November 1, 2013; date of current version November 20, 2013. This work was supported by the National Science Council of Taiwan under Contract NSC 101-2221-E-009-057-MY3. The review of this letter was arranged by Editor X. Zhou.

The authors are with the Department of Electronics Engineering and Institute of Electronics, National Chiao Tung University, Hsinchu 300, Taiwan (e-mail: chenmj@faculty.nctu.edu.tw).

Color versions of one or more of the figures in this letter are available online at http://ieeexplore.ieee.org.

Digital Object Identifier 10.1109/LED.2013.2286816

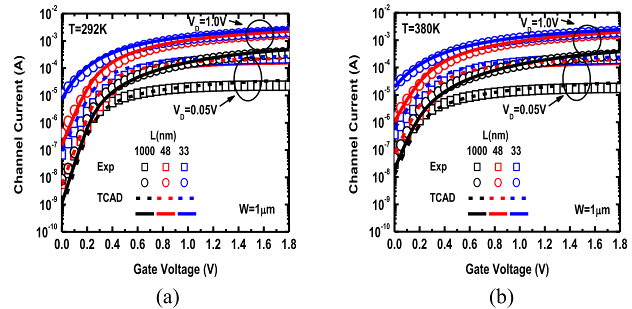

Fig. 1. Inverse modeling technique used to transform I–V's primarily in the subthreshold region into calibrated doping profiles. (a) 292 K. (b) 380 K.

In this letter, we propose a novel temperature-dependent method to probe long-range collective Coulomb interactions between channel electrons and source/drain plasmons. Aforementioned issues can be overcome with the method.

II. Experiment

Device samples presented are n^+ polysilicon ultrathin gate oxide (1.27-nm thick) n-channel MOSFETs having five channel lengths of 1 μm, 83, 48, 43, and 33 nm. The gate width is 1 μm. The p-type substrate doping concentration is 4×10^{17} cm^{-3}.The manufacturing process was described elsewhere [6]. I–V's are measured in a wide range of gate voltage up to 1.8 V, drain voltage of 0.05 and 1 V, and temperature of 292, 330, 360, and 380 K. Terminal currents of each sample measured across wafer change little.

Inverse modeling technique via TCAD Sentaurus [13] in its default conditions (i.e., the complete conventional scattering mechanisms due to ionized impurity, phonons, and surface roughness), along with the van Dort quantization model for quantum confinement, is employed to reproduce measured I–V's in the subthreshold region. We found that simulated subthreshold I–V's are largely sensitive to the positioning of both source/drain extensions and halo implants. The reproduction quality is fairly good as shown in Fig. 1, achieved without changing any physical parameters in TCAD. Resulting calibrated doping profiles are shown in Fig. 2.

Simulated inversion layer density N_{inv} as shown in Fig. 2 is used to transform measured above threshold drain current

0741-3106 © 2013 IEEE

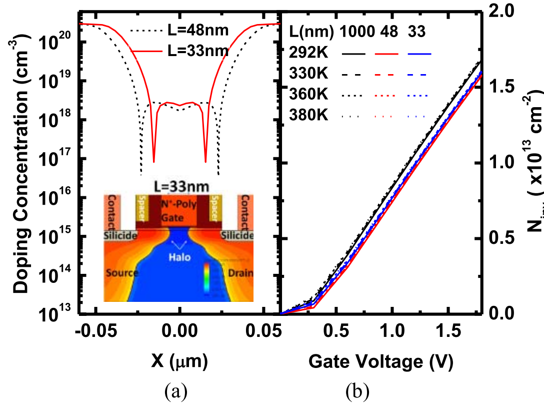

Fig. 2. Calibrated doping profiles from source extension through channel to drain extension, at a depth of 1.5 nm beneath the SiO_2/Si interface. Inset: calibrated structure of 33-nm channel length. (b) Simulated $N_{\rm inv}$ versus V_g with temperature as a parameter.

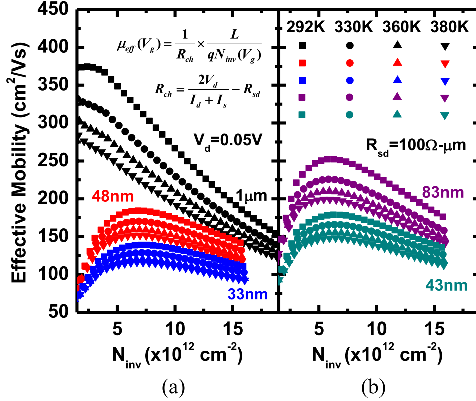

Fig. 3. Extracted electron effective mobility versus $N_{\rm inv}$ for (a) three and (b) two samples with the temperature as a parameter. Inset: formula to extract mobility. Source/drain series resistance $R_{\rm sd}$ is the total change in quasi-Fermi potential across both source and drain divided by the drain current. Because simulated $R_{\rm sd}$ is a weak function of temperature (from 99 Ω-μm at 292 K to 101 Ω-μm at 380 K), it is kept at 100 Ω-μm in this letter.

at $V_d = 0.05$ V into electron effective mobility. The result is shown in Fig. 3. In addition, simulated and measured threshold voltage values (~0.2 V) are close to each other. This means that the effect of increased channel doping on threshold voltage shift in short channel device (see Fig. 2) is considerably offset by corresponding short channel effect counterpart.

III. Additional Scatterers

With the application of Matthiessen's rule, effective mobility differences in Fig. 3 are transformed into the mobility components limited by additional scatterers, relative to 1-μm device, as shown in Fig. 4. It can be seen that additional scattering limited mobility of 43, 48, and 83 nm samples increases with both inversion layer density $N_{\rm inv}$ and temperature. For 33-nm case, however, mobility tends to saturate and decreases slightly with temperature. To highlight this, we add to the figure corresponding temperature dependencies at $N_{\rm inv} = 10^{13}$ cm^{-2}. Clearly, the temperature power law coefficient γ decreases with decreasing channel length and

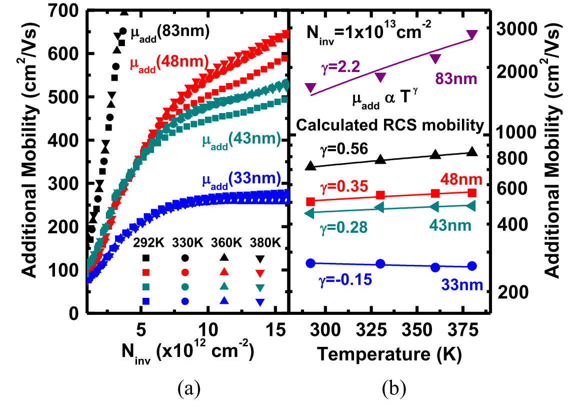

Fig. 4. Extracted additional scattering limited mobility (symbols) versus $N_{\rm inv}$ for four short channel samples, relative to 1 μm, with the temperature as a parameter. (b) Corresponding temperature dependencies at $N_{\rm inv} = 10^{13}$ cm^{-2}, along with calculated RCS limited mobility for comparison.

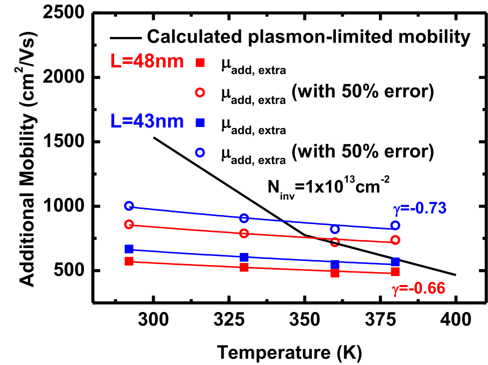

Fig. 5. Temperature dependence of extracted additional scattering limited mobility of 33-nm sample for two errors of $E_r = 0$ and 50%, relative to 43- and 48-nm ones. Calculated plasmon limited mobility is shown. Calculated and extracted plasmon limited mobility components separately refer to plasmons in 3-D doped silicon and plasmons in source/drain penetrating into the 2-D channel.

becomes negative at 33 nm. This dictates that the strength of source/drain plasmons increases with decreasing channel length. Relatively speaking, short-range Coulomb scattering or equivalently the remote Coulomb scattering [7], [9], and [14] weakens accordingly.

Mobility components of 33 nm with respect to 43 and 48 nm are further extracted with Matthiessen's rule. Corresponding temperature power-law coefficient γ is -0.66 and -0.73, repectively, as shown in Fig. 5. In the previous work [6], extracted mobility limited by interface plasmons has a γ of around -1, not differing much from those above. Other additional scatterers are relatively insignificant: 1) the ballistic mobility [15], because the presented samples are not short enough [16]; 2) the process altered surface roughness, because corresponding decreasing trend of mobility with $N_{\rm inv}$ does not exist in this letter (see Fig. 4); and 3) the process altered gate oxide thickness, because the measured gate currents per unit area do not differ much between samples (not shown here).

According to our previous work [12], extracted mobility in this letter is likely underestimated and must be corrected

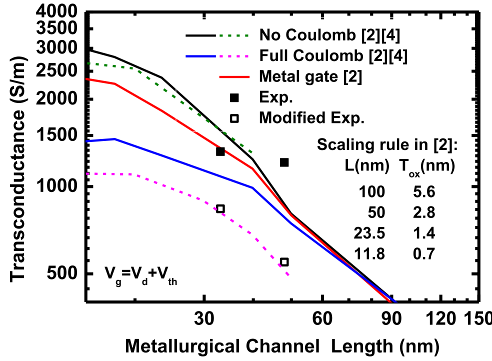

Fig. 6. Comparison of measured transconductance in this letter and those from 2-D [2] (solid lines) and 3-D [4] (dotted lines) simulations. The data are further changed such as to reflect the fact that gate oxide thickness in this letter is 1.27 nm, while in [2], it is ∼2.8- and 2-nm thick for 48 and 33 nm channel, respectively. Because the transconductance is essentially proportional to the equivalent gate oxide thickness, corresponding correction factor is made to be 1.27/2.8 and 1.27/2, respectively.

by multiplying a factor of $1 + E_r$ where E_r is the error. Fortunately, E_r remains unchanged if an adequate temperature range is selected [12] (292–380 K in this letter). This constitutes the merit of the proposed temperature-dependent method. The correction case is shown in Fig. 5. Obviously, the errors of Matthiessen's rule do not affect the resulting γ. Further, temperature dependence of RCS limited mobility is calculated directly quoting the literature formalism [17] (see [17, eqs. (11)–(15)]). Resulting γ is positive, as together plotted in Fig. 4 for a fixed charge density N_{fix} of 9×10^{13} cm^{-2} (close to those of [18] and [19] dedicated to long-channel devices with high-*k* dielectrics). Evidently, such high N_{fix} corresponds to a specific channel length between 48 and 83 nm, where the effect of source/drain plasmons is likely to be weak. Here, we attribute the used high N_{fix} to defects highly localized near source and drain of short channel devices [9] (also see the references therein), rather than the whole gate oxide [18], according to a recent literature [19]. Only in this situation, the calculated threshold voltage shift will not be so large. Indeed, noticeable threshold voltage change was not experimentally observed in this letter.

Further, 3-D electron plasmon scattering formalism [20] (see [20, eq. (18)]) was directly cited to calculate plasmon limited mobility in doped silicon. Such calculation is not quite straightforward due to the strong couplings with other scattering mechanisms such as impurity scattering, electron–electron scattering, and phonon scattering (see the source [20] for the comprehensive explanation). The result with a dopant concentration of 10^{20} cm^{-3} is shown in Fig. 5. The calculated and extracted plasmon limited mobility components exhibit the same descending trend with the temperature. Finally, we show in Fig. 6, a comparison between measured transconductance at large drain voltage and those of simulated ones [2], [4], plotted versus channel length. To make such comparison fair, the data in this letter are modified by considering the gate oxide thickness scaling [2]. Good agreements are evident, suggesting that source/drain plasmons actually prevail in shorter devices.

IV. Conclusion

We have experimentally probed long-range Coulomb interactions due to plasmons in source and drain. Corroborative evidence has thoroughly been established.

References

[1] D. Pines and D. Bohm, "A collective description of electron interactions: II. Collective vs individual particle aspects of the interactions," *Phys. Rev.*, vol. 85, no. 2, pp. 338–353, Jan. 1952.

[2] M. V. Fischetti and S. E. Laux, "Long-range Coulomb interactions in small Si devices. Part I: Performance and reliability," *J. Appl. Phys.*, vol. 89, no. 2, pp. 1205–1231, Jan. 2001.

[3] M. V. Fischetti, "Long-range Coulomb interactions in small Si devices. Part II: Effective electron mobility in thin-oxide structures," *J. Appl. Phys.*, vol. 89, no. 2, pp. 1232–1250, Jan. 2001.

[4] K. Nakanishi, T. Uechi, and N. Sano, "Self-consistent Monte Carlo device simulations under nano-scale device structures: Role of Coulomb interaction, degeneracy, and boundary condition," in *Proc. IEEE IEDM*, Dec. 2009, pp. 79–82.

[5] M. V. Fischetti, T. P. O'Regan, S. Narayanan, *et al.*, "Theoretical study of some physical aspects of electronic transport in nMOSFETs at the 10-nm gate-length," *IEEE Trans. Electron Devices*, vol. 54, no. 9, pp. 2116–2136, Sep. 2007.

[6] M. J. Chen, L. M. Chang, S. J. Kuang, *et al.*, "Temperature-oriented mobility measurement and simulation to assess surface roughness in ultrathin-gate-oxide (∼1 nm) nMOSFETs and Its TEM evidence," *IEEE Trans. Electron Devices*, vol. 59, no. 4, pp. 949–955, Apr. 2012.

[7] K. Rim, S. Narasimha, M. Longstreet, *et al.*, "Low field mobility characteristics of sub-100 nm unstrained and strained Si MOSFETs," in *Proc. IEDM*, Dec. 2002, pp. 43–46.

[8] A. Cros, K. Romanjek, D. Fleury, *et al.*, "Unexpected mobility degradation for very short devices: A new challenge for CMOS scaling," in *Proc. IEDM*, Dec. 2006, pp. 1–4.

[9] V. Barral, T. Poiroux, D. Munteanu, *et al.*, "Experimental investigation on the quasi-ballistic transport: Part II—Backscattering coefficient extraction and link with the mobility," *IEEE Trans. Electron Devices*, vol. 56, no. 3, pp. 420–430, Mar. 2009.

[10] F. Stern, "Calculated temperature dependence of mobility in silicon inversion layers," *Phys. Rev. Lett.*, vol. 44, no. 22, pp. 1469–1472, Jun. 1980.

[11] D. Esseni and F. Driussi, "A quantitative error analysis of the mobility extraction according to the Matthiessen rule in advanced MOS transistors," *IEEE Trans. Electron Devices*, vol. 58, no. 8, pp. 2415–2422, Aug. 2011.

[12] M. J. Chen, W. H. Lee, and Y. H. Huang, "Error-free Matthiessen's rule in the MOSFET universal mobility region," *IEEE Trans. Electron Devices*, vol. 60, no. 2, pp. 753–758, Feb. 2013.

[13] *TCAD Sentaurus, Version G-2012.06*, Synopsys, Mountain View, CA, USA, Jun. 2012.

[14] S. Saito, K. Torii, Y. Shimamoto, *et al.*, "Effects of remote-surface-roughness scattering on carrier mobility in field-effect-transistors with ultrathin gate dielectrics," *Appl. Phys. Lett.*, vol. 84, no. 8, pp. 1395–1397, Feb. 2004.

[15] M. S. Shur, "Low ballistic mobility in submicron HEMTs," *IEEE Electron Device Lett.*, vol. 23, no. 9, pp. 511–513, Sep. 2002.

[16] M. Zilli, D. Esseni, P. Palestri, *et al.*, "On the apparent mobility in nanometric n-MOSFETs," *IEEE Electron Lett.*, vol. 28, no. 11, pp. 1036–1039, Nov. 2007.

[17] N. Yang, W. K. Henson, J. R. Hauser, *et al.*, "Estimation of the effects of remote charge scattering on electron mobility of n-MOSFETs with ultrathin gate oxides," *IEEE Trans. Electron Devices*, vol. 47, no. 2, pp. 440–447, Feb. 2000.

[18] M. Cassé, L. Thevenod, B. Guillaumot, *et al.*, "Carrier transport in HfO_2/metal gate MOSFETs: Physical insight into critical parameters," *IEEE Trans. Electron Devices*, vol. 53, no. 4, pp. 759–768, Apr. 2006.

[19] P. Toniutti, P. Palestri, D. Esseni, *et al.*, "On the origin of the mobility reduction in n- and p-metal-oxide-semiconductor field effect transistors with hafnium-based/metal gate stacks," *J. Appl. Phys.*, vol. 112, no. 3, pp. 034502-1–034502-12, Aug. 2012.

[20] M. V. Fischetti, "Effect of the electron-plasmon interaction on the electron mobility in silicon," *Phys. Rev. B*, vol. 44, no. 11, pp. 5527–5534, Sep. 1991.